High static pressure alters spin trapping rates in solution. Dependence on the structure of nitrone spin traps

Yoshimi Sueishi,*[a] Daisuke Yoshioka,[a] Chiharu Yoshioka,[a] Shunzo Yamamoto[a] and Yashige Kotake[b,c]

Received 4th November 2005, Accepted 9th January 2006
First published as an Advance Article on the web 24th January 2006
DOI: 10.1039/b515682c

Using a competitive spin trapping method, relative spin trapping rates were quantified for various short-lived radicals (methyl, ethyl, and phenyl radicals). High static pressure was applied to the competitive spin-trapping system by employing high-pressure electron spin resonance (ESR) equipment. Under high pressure (490 bar), spin trapping rate constants for alkyl and phenyl radicals increased by 10 to 40%, and the increase was dependent on the structure of nitrone spin traps. A maximum increase was obtained when *tert*-butyl(4-pyridinylmethylene)amine *N*-oxide (4-POBN) was used as a spin trap. Activation volumes ($\Delta\Delta V^{\ddagger}$) for the two spin trapping reactions were calculated to be -17–(-9) cm^3 mol^{-1} for the 4-POBN system.

Introduction

The spin trapping technique has been widely used to understand reaction kinetics and mechanisms in chemical and biological free radical reactions.[1–4] The improvement of this technique may be accomplished by developing new spin traps that can produce spin adducts with longer half-lives.[3,5] However, our approach has been to change the thermodynamic parameters to alter reaction kinetics and equilibria.[6]

External pressure is a thermodynamic parameter that could control spin-trapping rates. Using a free radical probe and high-pressure ESR spectroscopy, we have demonstrated that high static pressure is a useful means for the manipulation of chemical equilibria.[7,8] We have also shown that spin-trapping rates were altered under high pressure.[6] In the present high-pressure study, we utilized various PBN (α-phenyl-*N*-*tert*-butylnitrone or benzylidene(*tert*-butyl)amine-*N*-oxide) type compounds as spin traps. Thus, three components, *i.e.*, the selected spin trap, the competing spin trap 2,2-dimethyl-3,4-dihydro-2*H*-pyrrole-1-oxide (DMPO), and free radical generating compound were mixed, and ESR spectrum was recorded under high pressure. Relative spin trapping rates were calculated by quantifying the yield of free radical adducts. The effects of substituents in PBN- and DMPO-analogs on alkyl and phenyl radical trapping rate constants were determined. We report that spin-trapping rates by various PBN- and DMPO-type traps are pressure dependent, and that the magnitude of pressure dependence is a function of the spin-trap structure.

Results and discussion

Determination of spin trapping rates

We employed a competitive spin-trapping method using two different spin traps.[4] Fig. 1a–b show the typical ESR spectra obtained from UV-irradiated solution of (a) trimethyllead acetate (methyl

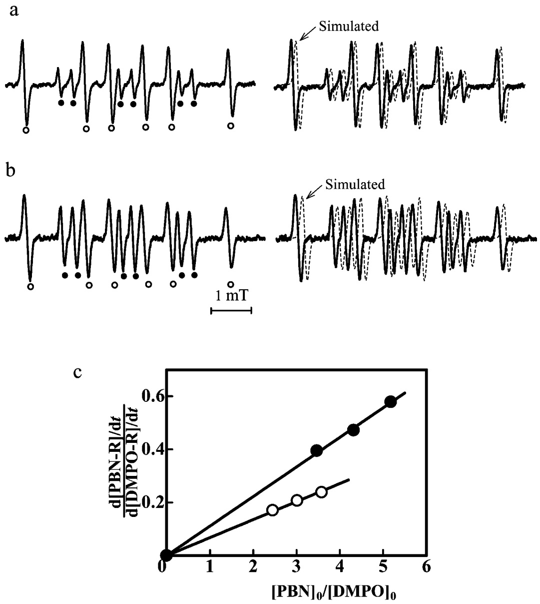

Fig. 1 ESR spectra obtained in aqueous solution immediately after UV-irradiation (irradiation time 1 s, sweep time 60 s) in the presence of DMPO and PBN. Broken lines in the spectra are computer simulated spectra: (a) methyl radical trapping; ○: DMPO-CH$_3$ and ●: PBN-CH$_3$. [PBN]$_0$: [DMPO]$_0$ (ratio of initial trap concentrations) was 3.6. (b) Ethyl radical trapping; ○: DMPO–C$_2$H$_5$ and ●: PBN–C$_2$H$_5$. [PBN]$_0$/[DMPO]$_0$ = 5.2. (c) The ratio of methyl (○) and ethyl-adduct (●) formation rates for PBN and DMPO, plotted as a function of the ratio of initial concentration of spin traps ([PBN]$_0$/[DMPO]$_0$).

---

[a] *Department of Chemistry, Faculty of Science, Okayama University, 3-1-1 Tsushima Naka, Okayama, 700-8530, Japan. E-mail: ysueishi@cc.okayama-u.ac.jp*
[b] *Free Radical Biology and Aging Research Program, Oklahoma Medical Research Foundation, Oklahoma City, OK, 73104, USA*
[c] *Kyoto University International Innovation Center, Uji, Kyoto, 611-0011, Japan*

radical source) and (b) triethyllead acetate (ethyl radical source) in the presence of the spin traps, DMPO and PBN. Two clearly identifiable spin adducts were obtained and peak assignments were made according to the reported ESR hyperfine splitting constants.[9] In Fig. 1, spectral lines marked with open circles are from DMPO spin-adducts (DMPO–CH_3) and closed circles are from PBN spin-adducts (PBN–CH_3). These ESR spectra were readily reproduced by computer spectrum simulations (Fig. 1). The relative abundance of the two spin adducts was calculated using the simulated spectra, from which relative spin-trapping rates were calculated (see the following paragraph). Thus, we carried out competitive spin-trapping for various PBN- and DMPO-type spin traps (Scheme 1) with DMPO as a reference spin trap. ESR parameters for alkyl radical spin-adducts trapped with PBN- and DMPO-analogs are listed in Table 1.

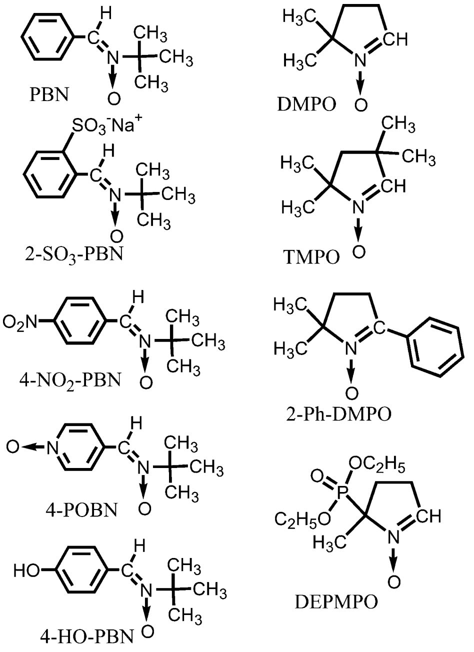

Scheme 1

The theoretical basis of the calculation of relative spin trapping rates from competitive spin trapping is as follows. The reaction scheme for spin trapping in the presence of two different traps (for example, PBN and DMPO) is:

$$(\mathrm{R})_3\,\mathrm{PbOAc} \xrightarrow{h\nu} \mathrm{R}^{\bullet}$$

$$\mathrm{DMPO} + \mathrm{R}^{\bullet} \xrightarrow{k_1} \mathrm{DMPO\text{-}R}$$

$$\mathrm{PNB} + \mathrm{R}^{\bullet} \xrightarrow{k_2} \mathrm{PBN\text{-}R}$$

The ratio of DMPO-R and PBN-R formation rates is expressed as follows:

$$\frac{R_{\mathrm{PBN}}}{R_{\mathrm{DMPO}}} = \frac{\mathrm{d[PBN\text{-}R]/d}t}{\mathrm{d[DMPO\text{-}R]/d}t} = \frac{k_2}{k_1}\frac{[\mathrm{PBN}]_0}{[\mathrm{DMPO}]_0} \qquad (1)$$

where $[\mathrm{PBN}]_0$ and $[\mathrm{DMPO}]_0$ denote the initial concentration of the spin traps. The relative rate constant (k_2/k_1) can be calculated from the relative rates of spin-adduct formation and the initial concentration of the spin-traps. Fig. 1c shows a typical plot for the PBN/DMPO system. In Fig. 1c, as predicted by eqn (1), the plot of $R_{\mathrm{PBN}}/R_{\mathrm{DMPO}}$ (the relative abundance of spin adducts) against $[\mathrm{PBN}]_0/[\mathrm{DMPO}]_0$ gives a straight line with the slope k_2/k_1 which passes through the origin, suggesting that the calculation of relative spin trapping rate constants (k_2/k_1) using eqn (1) is justifiable. The ratio of spin-trapping rate constants of methyl and ethyl radicals for various DMPO- and PBN-type traps are listed in Table 1.

Effect of spin-trap structure on spin-trapping rates (atmospheric pressure)

We determined the relative spin-trapping rate constants (k_2/k_1) of methyl and ethyl radicals for five PBN- and four DMPO-type spin traps as illustrated in Scheme 1. To demonstrate spin-trap structure dependence for methyl and ethyl radical trapping, we evaluated spin-trapping rate constants (k_2). Using time-resolved ESR spectroscopy, Taniguchi and Madden have determined the DMPO trapping rate constants in aqueous solution for various alkyl radicals produced with hydrogen abstraction by radiolytically-produced hydroxyl radicals, yielding $k_1 = 1.4 \times 10^7$ and 1.6×10^7 dm^3 mol^{-1} s^{-1} for methyl and ethyl radicals, respectively.[10]

Table 1 Hyperfine coupling constants (hfcc) and methyl and trapping rate constants for methyl and ethyl radicals at 298 K in aqueous solution

	Methyl adduct					Ethyl adduct					OH adduct[d]
	hfcc/mT					hfcc/mT					
Spin trap	a_H	a_N	a_P	k_2/k_1	$10^{-7}\ k_2$[a]	a_H	a_N	a_P	k_2/k_1	$10^{-7}\ k_2$[a]	$10^{-9}\ k_2$[a]
DEPMPO	2.260	1.542	4.820	2.15 ± 0.08	3.0	2.260	1.542	4.880	2.35 ± 0.05	4.0	6.16[e]
DMPO	2.380	1.650		1	1.4[b]	2.370	1.640		1	1.6[b]	3.60
4-NO_2-PBN	0.653	1.667		0.395 ± 0.017	0.55	0.310	1.628		0.462 ± 0.009	0.74	3.06
4-POBN	0.297	1.635		0.193 ± 0.004	0.27	0.280	1.590		0.566 ± 0.002	0.91	5.33
2-SO_3-PBN	0.360	1.670		0.0712 ± 0.0008	0.099	0.520	1.597		0.269 ± 0.002	0.43	4.82
TMPO	2.720	1.680		0.977 ± 0.001[c]	0.098	2.420	1.640		2.82 ± 0.01[c]	0.063	2.48[e]
PBN	0.340	1.660		0.0682 ± 0.0004	0.095	0.330	1.640		0.111 ± 0.014	0.18	2.56
4-HO-PBN	0.330	1.646		0.0589 ± 0.0055	0.082	0.320	1.647		0.0632 ± 0.0015	0.10	0.90
2-Ph-DMPO		1.600		0.0178 ± 0.0005	0.025		1.565		0.0133 ± 0.0005	0.021	1.58

[a] k_2 (dm^3 mol^{-1} s^{-1}). [b] Cited from ref. 10. [c] Ratio of trapping rate constants for PBN (k_2) and DMPO (k_1). [d] Cited from ref. 4. [e] Estimated using k_2/k_1 for the TMPO/PBN and DEPMPO/DMPO systems.

These DMPO trapping rate constants were utilized to calculate spin-trapping rate constants for the selected spin traps, and the results are listed in Table 1.

In our previous paper, we proposed that the nucleophilic attack of hydroxyl and phenyl radicals may occur against the C=N double bond in nitrone traps.[4] To evaluate the effects of the spin-trap structure on the trapping rate constants of alkyl radicals, the Hammett plot may be useful. However, substituent constants for the 2-subtituent in 2-SO_3-PBN and N→O group in the phenyl ring of 4-POBN are not available. Therefore, alternatively we plotted the spin trapping rate constants of alkyl radicals against those of the hydroxyl radical (Fig. 2). Fig. 2 clearly shows the tendency that an electron-withdrawing group tends to increase PBN(-type) trapping rate constants of alkyl radicals, suggesting that there was nucleophilic addition similar to the case of hydroxyl and phenyl radical trapping.[4] Table 1 also shows that spin-trapping rate constants by TMPO and 2-Ph-DMPO are extremely small compared with those of DMPO and DEPMPO. Such a decrease cannot be attributed to the electron-inductive effect on spin trapping, but rather to the steric hindrance by methyl and phenyl groups around the trapping site (nitrone group). This is in agreement with the results obtained for hydroxyl and phenyl radical trapping by TMPO and 2-Ph-DMPO.[4]

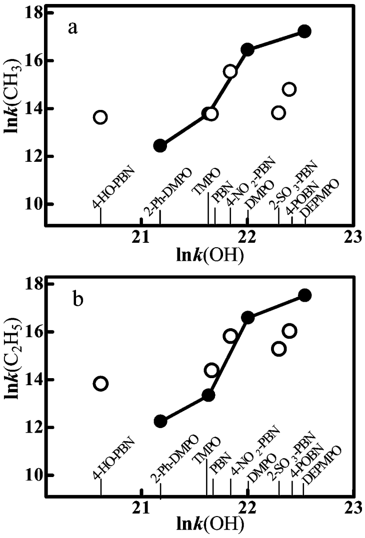

Fig. 2 Plots of spin-trapping rate constants of (a) methyl and (b) ethyl radicals against trapping rate constants of hydroxyl radical; ○: PBN- and ●: DMPO-type traps.

Pressure effects on spin-trapping reaction

Effects on reaction rates. Under a pressure of 490 bar, methyl or ethyl radicals were produced in a UV-irradiated solution of trimethyllead acetate or triethyllead acetate in the presence of DMPO and 4-POBN. The relative rates of methyl radical trapping clearly increased at 490 bar, as indicated by the change in the intensity ratio between the lines marked with arrows in Fig. 3a. The relative rate constants (k_2/k_1) at 490 bar are quantified according to eqn (1), and the results are listed in Table 2. Percent changes in relative trapping rate constants (= $100((k_2/k_1)^{490} - (k_2/k_1)^1)/(k_2/k_1)^1$) induced by 490 bar are listed in Table 2. The percentage induction in the 4-POBN/DMPO system is larger than others.

Activation volumes and transition states. Based on the pressure dependence on the relative rate constants (Table 1), we evaluated the difference in activation volumes ($\Delta\Delta V^\ddagger$) for the two trapping activation processes according to the following equations:

$$\ln(k_2/k_1) = aP + b, \tag{2}$$

$$\Delta\Delta V^\ddagger = -RT\left(\frac{\mathrm{d}\ln(k_2/k_1)}{\mathrm{d}P}\right)_\mathrm{T} = \Delta\Delta V^\ddagger_{\mathrm{PBN-type}} - \Delta\Delta V^\ddagger_{\mathrm{DMPO-type}} \tag{3}$$

The calculated values for $\Delta\Delta V^\ddagger$ are given in the right hand side column in Table 2.

As indicated in Table 2, in alkyl and phenyl radical trapping, $\Delta\Delta V^\ddagger$ values are negative. It is noted that the $|\Delta\Delta V^\ddagger|$ values (= 9–17 cm^3 mol^{-1}) for alkyl and phenyl radical trapping in the 4-POBN/DMPO system are obviously larger than others.

Table 2 External pressure dependence of relative spin trapping rate constants and activation volumes at 298 K

Traps[a]	Radical	Solvent[b]	k_2/k_1				Ratio[d]	$\Delta\Delta V^\ddagger$
			1 bar	98 bar	245 bar	490 bar[c]		cm^3 mol^{-1}
4-POBN/DMPO	Phenyl[e]	B	0.64 ± 0.02	0.69	0.77	0.89	39	−17 ± 1
4-POBN/DMPO	Methyl	W	0.193 ± 0.004	0.208	0.234	0.259	34	−16 ± 1
4-POBN/2-Ph-DMPO	Phenyl	B	1.21 ± 0.01	1.23	1.36	1.44	19	−9.3 ± 1.2
4-POBN/DMPO	Ethyl	W	0.566 ± 0.002	0.581	0.625	0.675	19	−8.9 ± 0.5
4-POBN/DMPO	Hydroxyl[e]	W	1.45 ± 0.16	1.39	1.44	1.43	1	0.17 ± 0.05
PBN/DMPO	Methyl	W	0.0682 ± 0.0004	0.0711	0.0761	0.0870	28	−12 ± 1
PBN/DMPO	Ethyl	W	0.111 ± 0.014	0.112	0.115	0.118	6	−4.1 ± 0.2
2-Ph-DMPO/DMPO	Methyl	W	0.0178 ± 0.0005	0.0185	0.0193	0.0212	19	−8.8 ± 0.3
2-Ph-DMPO/DMPO	Ethyl	W	0.0133 ± 0.0005	0.0140	0.0144	0.0157	18	−8.0 ± 0.5
2-Ph-DMPO/DMPO	Phenyl[e]	B	0.59 ± 0.03	0.63	0.65	0.69	17	−7.8 ± 0.3
2-Ph-DMPO/DMPO	Hydroxyl[e]	W	0.51 ± 0.01	0.52	0.53	0.53	4	−2.3 ± 0.3
2-SO_3-PBN/DMPO	Methyl	W	0.0712 ± 0.0008	0.0739	0.0787	0.0849	19	−9.2 ± 0.4
2-SO_3-PBN/DMPO	Ethyl	W	0.269 ± 0.002	0.279	0.292	0.305	13	−6.9 ± 0.6
4-NO_2-PBN/DMPO	Phenyl	B	1.76 ± 0.02	1.94	2.02	2.21	26	−11 ± 1
PBN/TMPO	Methyl	W	0.977 ± 0.001	1.01	1.02	1.03	5	−2.2 ± 0.1
PBN/TMPO	Ethyl	W	2.82 ± 0.01	2.74	2.63	2.49	12	6.5 ± 0.8

[a] The solubility of 4-NO_2-PBN in water and 2-SO_3-PBN in benzene is low, thus some combinations are missing from this list. [b] W: water; B: benzene. [c] 1 bar = 1 × 10^5 Pa [d] Ratio = $100((k_2/k_1)^{490} - (k_2/k_1)^1)/(k_2/k_1)^1$. [e] Cited from ref. 6.

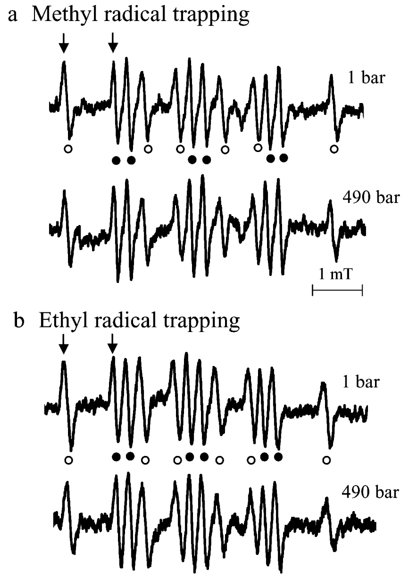

Fig. 3 ESR spectra obtained in aqueous solution immediately after UV-irradiation (irradiation time 1 s, sweep time 60 s) in the presence of 4-POBN and DMPO at 1 and 490 bar. (a) Methyl radical trapping; ○: DMPO-CH_3 and ●: 4-POBN-CH_3. $[\text{4-POBN}]_0/[\text{DMPO}]_0 = 3.0$. [4-POBN-$CH_3$] : [DMPO-$CH_3$] was 0.579 and 0.777 at 1 and 490 bar, respectively. (b) Ethyl radical trapping; ○: DMPO-C_2H_5 and ●: 4-POBN-C_2H_5. $[\text{4-POBN}]_0/\text{DMPO}]_0 = 1.3$. [4-POBN-$C_2H_5$] : [DMPO-$C_2H_5$] was 0.736 and 0.878 at 1 and 490 bar, respectively.

$|\Delta\Delta V^{\ddagger}|$ values in the other PBN analogs are in the range of 4 to 12 cm^3 mol^{-1} for alkyl and phenyl radicals, but the pressure dependence of hydroxyl radical trapping rates was negligibly small[6] (Table 2).

The activation volume for chemical reactions is conventionally divided into two terms: intrinsic ($\Delta V^{\ddagger}_{\text{int}}$) and solvational ($\Delta V^{\ddagger}_{\text{sol}}$) part, *i.e.*

$$\Delta V^{\ddagger} = \Delta V^{\ddagger}_{\text{int}} + \Delta V^{\ddagger}_{\text{sol}} \tag{4}$$

Usually, the intrinsic volume change ($\Delta V^{\ddagger}_{\text{int}}$) for the addition reaction of neutral radical molecules is a negative value, and the volume change ($\Delta V^{\ddagger}_{\text{sol}}$) due to solvation is negligible. From the pressure dependence on the relative trapping rates, the difference in activation volumes for two trapping processes ($\Delta\Delta V^{\ddagger}$) can be expressed as follows:

$$\Delta\Delta V^{\ddagger} = \Delta\Delta V^{\ddagger}_{\text{int}} + \Delta\Delta V^{\ddagger}_{\text{sol}} \tag{5}$$

In chemical reaction in solution, steric crowding causes lower a partial volume than non-crowded species because the reaction that proceeds through sterically-hindered transition state could result in a substantial loss of freedom of internal rotation of the mutually-repelling groups of atoms.[11,12] Such difference could cause substantial decrease in the free volume.

Negative $\Delta\Delta V^{\ddagger}$ values in Table 2 suggest that the degree of steric crowding in the transition state for PBN-analog or 2-Ph-DMPO spin-trapping is higher than that in DMPO spin-trapping. Scheme 2 illustrates how steric crowding influences the magnitude of $|\Delta\Delta V^{\ddagger}|$. This is also supported from the visual inspection of the Corey–Pauling–Koltun (CPK) space-filling model (this figure is not shown). Gonikberg *et al.*[13,14] have shown that phenyl radical addition to 2- or 4-position of *t*-butylbenzene, the product ratio (2-position addition : 4-position addition) increased with rising pressure. Furthermore, the $\Delta\Delta V^{\ddagger}$ value for the additions to the two positions was reported to be $\Delta\Delta V^{\ddagger} = -8$ cm^3 mol^{-1}.[13] This is in good agreement with our present observation for competitive trapping of alkyl- and phenyl-radicals in the PBN analogs and 2-Ph-DMPO systems (4–12 cm^3 mol^{-1}), suggesting that the trapping proceeds through crowded transition states. It should be emphasized that $|\Delta\Delta V^{\ddagger}|$ values for the 4-POBN/DMPO system are large as compared with the others (Table 2). We calculated the difference in the activation volumes for trapping processes by 4-POBN and PBN using the $\Delta\Delta V^{\ddagger}$ values in Table 2 and the following equation.

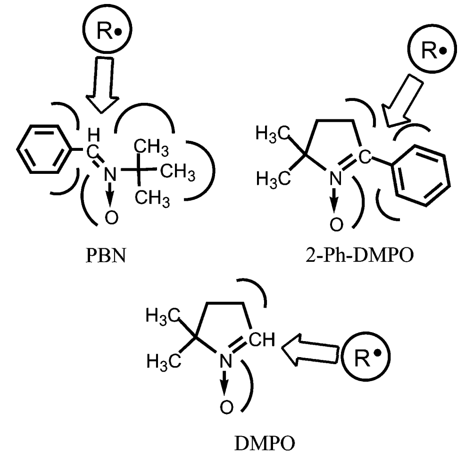

Scheme 2

$$\begin{aligned}\Delta\Delta V^{\ddagger}_{\text{4-POBN/PBN}} &= \Delta V^{\ddagger}_{\text{4-POBN}} - \Delta V^{\ddagger}_{\text{PBN}} \\ &= \Delta\Delta V^{\ddagger}_{\text{4-POBN/DMPO}} - \Delta\Delta V^{\ddagger}_{\text{PBN/DMPO}}.\end{aligned} \tag{6}$$

The $\Delta\Delta V^{\ddagger}_{\text{4-POBN/PBN}}$ values for methyl- and ethyl-trappings are calculated to be −4.0 and −4.8 cm^3 mol^{-1}, respectively. These values suggest that the spin-trapping reaction with 4-POBN involves the presence of extra volume constriction as compared with PBN. We consider that the N→O group in the POBN phenyl ring contributes to the negative $\Delta\Delta V^{\ddagger}_{\text{4-POBN/PBN}}$ value (*ca.* −5 cm^3 mol^{-1}). Scheme 3 shows the canonical resonance structures of 4-POBN with formal charges on the nitrogen and oxygen atoms, resulting in the delocalization of the π-electrons. Upon

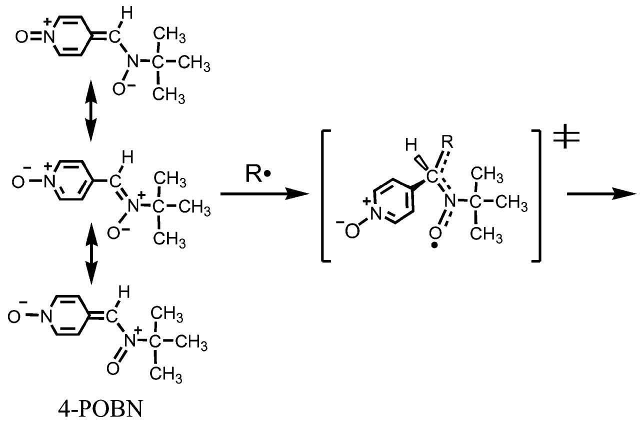

Scheme 3

radical-trapping with 4-POBN, the twist of the phenyl moiety causes a reduction in the resonance contribution, and the polarity of the transition state will increase. Thus, the negative value of $\Delta\Delta V^{\ddagger}_{\text{4-POBN/PBN}}$ can be explained in terms of the change in volume ($\Delta\Delta V^{\ddagger}_{\text{sol}}$) due to solvation for the polar activation complex of 4-POBN spin trapping.

In PBN analogs, $|\Delta\Delta V^{\ddagger}|$ for methyl radical trapping is larger than those for ethyl radical, *i.e.*, $|\Delta\Delta V^{\ddagger}(\mathrm{CH_3}^{\bullet}) - \Delta\Delta V^{\ddagger}(\mathrm{C_2H_5}^{\bullet})| =$ 7.1, 7.9, and 2.3 $\mathrm{cm^3\ mol^{-1}}$ for 4-POBN/DMPO, PBN/DMPO, and 2-$\mathrm{SO_3}$-PBN/DMPO, respectively. From Table 1, we notice that methyl-radical trapping rate constants by DMPO analogs are similar to those of ethyl radical. Taniguchi and Madden,[10] in their kinetic spin trapping study, suggested that spin trapping rate constants are usually influenced by both electronic and steric factors, but DMPO did not exhibit the strong electronic character in their study. In the present study, methyl radical trapping rate constants by PBN analogs are smaller than ethyl radical (Table 1), indicating that the electronic factor is operative in the case of PBN analogs. The difference in the methyl and ethyl radical trapping rate constants by PBN analogs may be attributed to the difference in the activation energy for the trapping reaction. According to the Hammond postulate,[15] the transition state for the reaction with a large activation energy should be product-like in terms of energy and geometry. Therefore, we may assume that the methyl and ethyl trapping reactions by DMPO analogs have similar transition-state structures, while the transition state for the methyl radical trapping by PBN analogs lies closer to the product as compared with that of ethyl radical trapping. This could give rise to the larger negative $\Delta V^{\ddagger}$ value for methyl radical trapping by PBN. In contrast, for 2-Ph-DMPO/DMPO and TMPO/DMPO($= \Delta\Delta V^{\ddagger}_{\text{PBN/DMPO}} - \Delta\Delta V^{\ddagger}_{\text{PBN/TMPO}}$) systems, the $\Delta\Delta V^{\ddagger}$ values for methyl radicals are comparable to ethyl radical. Again, this supports our interpretation.

In summary, we show the large effect of external pressure on the spin-trapping reactions of methyl, ethyl, and phenyl radicals. Pressure-induced acceleration in trapping rates is more pronounced in systems that can form sterically-hindered trapping sites. We believe that the external pressure could be a useful factor that can effectively control the rate of spin-trapping reactions.

Experimental

Materials

Spin traps used are shown in Scheme 1: benzylidene(*tert*-butyl)-amine-*N*-oxide (PBN), sodium *tert*-butyl(2-sulfonatobenzylidene)-amine-*N*-oxide (2-$\mathrm{SO_3}$-PBN), *tert*-butyl(4-nitorobenzylidene)-amine-*N*-oxide (4-$\mathrm{NO_2}$-PBN), *tert*-butyl(4-pyridinylmethylene)-amine-*N*-oxide (4-POBN), *tert*-butyl(4-hydroxybenzylidene)amine-*N*-oxide (4-HO-PBN), 2,2-dimethyl-3,4-dihydro-2*H*-pyrrole-1-oxide (DMPO), 2,2,4,4-tetramethyl-3,4-dihydro-2*H*-pyrrole-1-oxide (TMPO), 2,2-dimethyl-5-phenyl-3,4-dihydro-2*H*-pyrrole-1-oxide (2-Ph-DMPO), and 2-(diethoxyphosphoryl)-2-methyl-3,4-dihdro-2*H*-pyrrole-1-oxide (DEPMPO). DEPMPO was purchased from Radical Research Inc. (Hino, Japan), and 4-HO-PBN was synthesized in the OMRF laboratory. Other PBN- and DMPO-type traps were obtained from Aldrich Chemical Company, Inc. (Milwaukee WI, USA). Trimethyllead acetate, triethyllead acetate, tetraphenyllead and hydrogen peroxide (30%) were obtained from Wako Pure Chemicals (Osaka, Japan), and were used as sources of methyl, ethyl, phenyl and hydroxyl radicals. Benzene and water were purified by distillation.

ESR measurements of free radical (spin) adducts

A competitive spin trapping method was used to determine relative spin trapping rates. The competitor spin trap was DMPO except when the counterpart was TMPO. A JEOL-FE3XG spectrometer equipped with a 100 kHz field modulator was used for the ESR measurements. Methyl and ethyl radicals were generated with UV-irradiation (200 W mercury arc RUVF-203S, Radical Research Inc., Hino, Japan). For instance, trimethyllead acetate (5×10^{-3} mol $\mathrm{dm^{-3}}$) and spin traps ($5\text{–}10 \times 10^{-3}$ mol $\mathrm{dm^{-3}}$) were mixed in water and loaded in the ESR flat cell. The sample solution was set inside the ESR cavity. ESR signals were recorded immediately after UV irradiation: irradiation time 1 s, sweep time 60 s, time constant 0.3 s, microwave power 5 mW. ESR spectra of two different spin-adducts were computer-simulated with the aid of an attached computer program (WIN-RAD computer system, Radical Research Inc., Hino, Japan) by adjusting the relative intensity of the two radical adducts. The relative abundance (concentration) of the two components was calculated as follows: 1) obtain a best-fit simulated spectrum, and 2) using simulated component spectra, calculate the relative abundance of the two components with a computer-mediated double-integration routine of the first-derivative signal of each component. The plot of the relative abundance of spin-adducts against initial concentrations of spin-traps gives a line with the slope k_2/k_1. In case of TMPO, because the ESR signal of TMPO spin-adduct overlapped with DMPO adduct, we used PBN as a competitor trap instead of DMPO.

In order to confirm that spin-adduct decay would not influence the trapping rate measurement, we monitored the decay rate of the spin adducts. Time-dependent decrease of ESR peak heights was measured for PBN-$\mathrm{CH_3}$, PBN-$\mathrm{C_2H_5}$, DMPO-$\mathrm{CH_3}$, and DMPO-$\mathrm{C_2H_5}$ in aqueous solution at 298 K. The results indicated that all the decay was first-order, and half-lives are 3.1, 1.8, 1.2 and 1.2 × 10^3 s, respectively. Other PBN-type adducts showed longer half-lives than PBN-$\mathrm{CH_3}$. Because spin-trapping rates are much higher

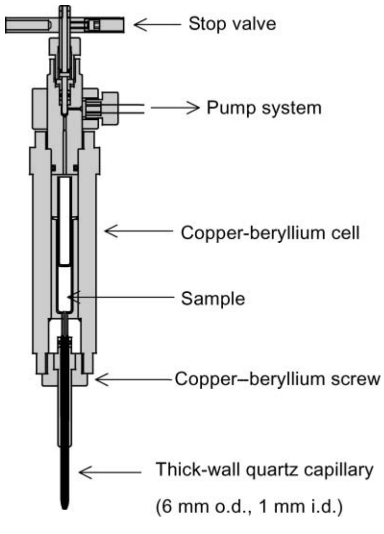

Fig. 4 High-pressure cell for ESR measurement.

than the spin-adducts' decay rates,[10] we concluded that the decay did not interfere with spin-trapping rate measurements.

EPR signals from all described spin-trapping systems were recorded at 1 bar (atmospheric pressure) and high pressure (*ca.* 490 bar). Procedures for ESR measurements at high pressure were the same as those described elsewhere.[7] A diagram of the high-pressure ESR system is shown in Fig. 4. A thick-wall quartz capillary tubing (i.d. 1 mm and o.d. 6 mm) was used as a sample cell, and the sample tube packed with chemicals was fitted to a manual static pressure generator (Model KP3W, Hikari Kouatsu Inc., Hiroshima, Japan) through a Heise–Bourdon gauge and a small stop-valve. After applying pressure, the stop valve was closed and the cell was disconnected from the high-pressure pump system and set into the ESR cavity. UV light was illuminated to the pressurized sample *in situ* and ESR signals were recorded immediately after the UV illumination.

References

1 E. G. Janzen, *Acc. Chem. Res.*, 1977, **4**, 31.
2 F. A. Villamena, C. M. Hadad and J. L. Zweier, *J. Am. Chem. Soc.*, 2004, **126**, 1816.
3 F. Chalier and P. Tordo, *J. Chem. Soc., Perkin Trans. 2*, 2002, 2110.
4 Y. Sueishi, C. Yoshioka, C. Olea-Azar, L. A. Reinke and Y. Kotake, *Bull. Chem. Soc. Jpn.*, 2002, **75**, 2043.
5 V. Roubaud, H. Dozol, C. Rizzi, R. Lauricella, J. C. Bouteiller and B. Tuccio, *J. Chem. Soc., Perkin Trans. 2*, 2002, 958.
6 C. Yoshioka, Y. Kotake and Y. Sueishi, *Chem. Phys. Lett.*, 2004, **385**, 189.
7 Y. Sueishi, H. Tobisako and Y. Kotake, *J. Phys. Chem. B*, 2004, **108**, 12623.
8 Y. Sueishi, H. Inoue, T. Oka, H. Tsukube and S. Yamamoto, *Bull. Chem. Soc. Jpn.*, 1998, **71**, 817.
9 G. R. Buettner, *J. Free Radicals Biol. Med.*, 1987, **3**, 259.
10 H. Taniguchi and K. P. Madden, *J. Am. Chem. Soc.*, 1999, **121**, 11875.
11 N. S. Isaacs, *Liquid Phase High Pressure Chemistry*, John Wiley & Sons, New York, 1981.
12 A. Drljaca, C. D. Hubbard, R. van Eldik, T. Asano, M. V. Basilevsky and W. J. le Noble, *Chem. Rev.*, 1998, **98**, 2167.
13 M. G. Gonikberg, *High Pressure Chemistry*, Nikkan Kogyo Shimbun, Tokyo, 1972.
14 M. G. Gonikberg, N. I. Prokhorova and E. F. Litvin, *Dokl. Akad. Nauk SSSR*, 1963, **148**, 105.
15 G. S. Hammond, *J. Am. Chem. Soc.*, 1955, **77**, 334.